www.cadanda.com
Computer-Aided Design AND APPLICATIONS

Using Parametric Effectiveness for Efficient CAD-Based Adjoint Optimization

Dheeraj Agarwal[1], Kapellos Christos[2], Trevor T. Robinson[3] and Cecil G. Armstrong[4]

[1]Queen's University Belfast, d.agarwal@qub.ac.uk
[2]Volkswagen Research, Germany, christos.kapellos@volkswagen.de
[3]Queen's University Belfast, t.robinson@qub.ac.uk
[4]Queen's University Belfast, c.armstrong@qub.ac.uk

Corresponding author: Trevor T. Robinson, t.robinson@qub.ac.uk

ABSTRACT

Parametric effectiveness is a measure of the ability of the parameters defining a CAD model to be used for optimization. It compares the optimum change in performance that can be achieved using a CAD model's parameterization, to the maximum performance improvement that could be obtained if the model is free to move. The aim of this paper is to present an automated approach to efficiently compute the parametric effectiveness for the parameters defined within a CAD modelling software CATIA V5. The approach is further developed to automatically identify a subset of CAD parameters which provides the greatest potential for performance improvement. The rationale for selecting such a subset is to reduce the time required to update a parametric CAD model during the optimization, which is an important factor to be considered in an industrial workflow. The approach is applied to the shape optimization of an S-Bend duct for minimizing the power-loss and an automotive car mirror for minimizing the noise perceived by the driver of the car. The flow sensitivities are computed with a continuous adjoint method.

Keywords: parametric effectiveness, adjoint method, design velocity, CAD, parameters.
DOI: https://doi.org/10.14733/cadaps.2019.703-719

1 INTRODUCTION

With advances in the field of computers and their increasing use within the industrial design process, the need for the physical design prototypes has been extensively reduced and replaced with digital models which are constructed and analysed using computers. Nowadays product design typically starts with a Computer-aided design (CAD) geometry of an initial concept and the goal is to deliver an optimized geometry in CAD which is used for manufacturing. There is a desire to use CAD model parameters as design variables for optimization, but one of the key issue restricting this ambition is

that there is no clear link between the CAD parameters and how these parameters effect the model's performance. Thus, researchers tend to use the nodes of the computational mesh [5],[12],[16],[17] as design variables. One major drawback for this parameterization strategy is that, as all surface mesh nodes can move independently, the implementation of a smoothing algorithm is required to prevent the appearance of non-smooth shapes that often appear in the model during the optimization process. Other methods, such as level-sets which work on the computational mesh to alter the topology of the model [13],[14],[35], produce solutions which are not CAD-compatible.

To achieve the link between CAD geometries and optimization, researchers have used methodologies including the use of non-uniform rational B-splines (NURBS) and feature-based CAD models. A NURBS patch can be defined as

$$X_s(u,v) = \sum_{i=0}^{n}\sum_{j=0}^{m} P_{i,j}B_{i,j}(u,v)\,, \tag{1.1}$$

where $P_{i,j}$ are the position of NURBS control points, and $B_{i,j}(u,v)$ is the basis function defined as

$$B_{i,j}(u,v) = \frac{N_{i,p}(u)N_{j,q}(v)w_{i,j}}{\sum_{k=0}^{n}\sum_{l=0}^{m} N_{k,p}(u)N_{l,q}(v)w_{k,l}}, \tag{1.2}$$

where $N_{i,p}(u)$ and $N_{j,q}(v)$ are the p-th and q-th degree basis functions defined on (u,v) parametric space. Some authors [6],[26],[36],[38],[39] have attempted to develop the optimization processes based on NURBS patches, where the NURBS control point locations are used as design variables. In order to increase the applicability of the NURBS with multiple patches, the approaches have been developed to enforce continuity constraints along the patch interfaces [36]. Recent work by Xu et al. [37] has extended NURBS parametrization method to include geometric constraints such as thickness and trailing edge radius. One downside of using NURBS is that sometimes the NURBS control net may be too coarse in certain regions and would require a process to enrich the control net by adding more control points before it is used for optimization. Rejish et al. [18] presented an adaptive parameterization approach based on NURBS patches, where the NURBS control net was refined by using knot insertion, and subsequently used to optimize the pressure loss across a U-Bend passage of a turbine blade serpentine cooling passage. Koch et al. [23] used NURBS curve to define the level-set boundary and subsequently used it for the shape optimization. The approach demonstrated a link between the 2D level-set topology results and CAD-based shape optimization methods, its extension to 3D models is a challenging task.

Modern CAD systems like CATIA V5, SIEMENS NX, SolidWorks etc. use feature-based modelling strategies to create a parametric CAD model. While many CAD systems are capable of constructing NURBS geometry through the use of CAD features, by editing the NURBS definition directly all the information about which CAD features were used to build the model are lost, and in many cases the design intent for the model is inherent in these features. For feature-based CAD models, the shape of the model can also be updated by changing the values of the parameters defining different features used to create the model. The benefit of this approach is that, assuming the original model was well created, the constraints on the shape imposed by the features in the CAD model feature tree would mean that the optimized part can be manufactured. To a large extent this will depend on the skill and experience of the CAD model creator, and their ability to visualize and parameterize the design space. The downside of using a feature-based CAD model to optimize the design is that the parameters are not primarily chosen with optimization in mind, and often it is not obvious from the parameterization which parameter value(s) need to be modified to achieve the desired shape change, especially when the person implementing the change is not the creator of the CAD model.

In this work, gradient based optimization methods are used for shape optimization. This requires an efficient methodology for the computation of the gradient of objective function as well as the constraints (if any) with respect to design variables. The most straight forward route of calculating these gradients is by employing finite differences, the benefit being that it is simple to implement. However, the industrial feasibility of this approach is limited by the associated computational cost of computing additional function values which scale with the number of design variables. In the pursuit of efficient gradient calculations, adjoint based techniques have shown promising results. They have

been an area of extensive research over the last two decades, especially for the aerodynamic optimization [9],[15],[25]. The applicability of adjoint methods has been demonstrated in turbo-machinery [19],[29],[34] and the automotive industry [27],[33]. The underlying principle of adjoint methods is the computation of adjoint sensitivities i.e. the derivative of objective function with respect to design parameters. Adjoint surface sensitivities give information about how the objective function changes for an infinitesimally small movement of each surface mesh node in the normal direction. The primary attraction of adjoint methods is their ability to compute gradient information at a computational cost which is essentially independent of the number of design parameters. This, in turn, opens up the possibility to explore significantly larger design spaces than those with traditional approaches, in time-scales which are acceptable for industrial design.

Parametric design velocity quantifies the boundary movement with respect to a change in the parameter value. This measure was first developed in the context of structural optimization [7]. Robinson et al. [32] used adjoint sensitivities and design velocities to define the measure of parametric effectiveness to rate the quality of CAD parameterizations to be used for optimization. Parametric effectiveness compares the maximum performance improvement that can be achieved using the model's parameterization, to the maximum performance improvement that could be obtained if the model is free to move (i.e. not constrained by any parameterization), where both are subjected to the constraint of a unit root-mean-squared boundary movement. The aim of this paper is to present an automated approach to efficiently calculate the parametric effectiveness for any set of parameters defined within a CAD modelling system CATIA V5. In this work, the approach is also used to automatically select a subset of parameters which provides the greatest potential for performance improvement, while reducing the optimization time through the reduction in design variables. The ability to down-select to the most effective set of parameters is advantageous because while one of the benefits of adjoint optimization is that the cost of calculating gradients is virtually independent of the number of design parameters, the cost of modifying a CAD model of industrial complexity by changing all parameters during an optimization step is potentially high.

The remainder of the paper will first summarize the theory of design velocity, continuous adjoint method and parametric sensitivity computation. This will be followed by the methodology to compute parametric effectiveness and select the most effective subset of parameters. The results on three automobile test cases will be presented and discussed. The paper will finish with the conclusions.

2 THEORY

2.1 Design velocity

In a feature-based CAD modelling system (e.g. CATIA V5 which is a popular industrial CAD system), a part model is comprised of individual features which are combined to represent an overall shape. In order to capture the CAD surface movement with respect to the change in CAD parameters, the design velocity is calculated. This is the movement of the CAD model boundary in the normal direction due to a change in the parameter value, and can be formulated as

$$V_n = \delta X_s \cdot \hat{n}, \tag{2.1}$$

where δX_s is the movement of surface points and $\hat{n}$ is the outward unit normal of the surface at that point. For each location on the domain boundary, the design velocity is represented by a scalar value. In Figure 1, the arrows represent the design velocity as the boundary changes from solid line to the dashed line. The convention adopted throughout this work is that a positive design velocity represents an outward movement of the boundary, and negative is inward.

The design velocities of the CAD model are calculated using the approach described by Agarwal *et. al*. [4] and is in effect a finite difference on the shape of the 3D CAD models before and after the parameter perturbation. The implementation process includes computing the geometrical movement along the normal direction between two discrete representations of the original and perturbed geometries. The process incorporates various CAD design software tools by using a generic STEP representation of CAD model as the input. Note that STEP files are part of the computation process,

but the fully featured CAD file is maintained throughout. Its reliance on CAD means that it can be easily integrated to most industrial optimization workflows (regardless of CAD system) and is immune to the topology and labelling issues highlighted by other CAD based optimization processes [10],[24].

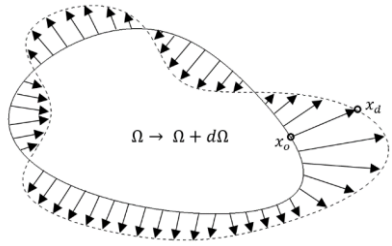

Figure 1: A two-dimensional design velocity field.

2.2 Continuous adjoint method

In this work, the continuous adjoint method is used to compute the gradient of the objective function with respect to surface normal displacement, at a computational cost practically independent of the number of design variables. To do so, the adjoint system of equations is solved, which is similar to the state equations, here the incompressible Navier-Stokes equations. The adjoint equations, their boundary conditions and the final expression of the gradient, namely the sensitivity derivative, are derived by differentiating the objective function augmented by the volume integrals of the primal equations multiplied by the adjoint variables. The adjoint equations are then discretized similarly to the primal equations and solved to compute the objective function gradient. The computed adjoint sensitivity map show how the geometry shape should change in the normal to the surface direction, in order to achieve a reduction in the objective function, and they can be combined with the design velocity, as in Eqn. (2.2), to calculate the total derivative of the objective function with respect to the CAD parameters.

2.3 Parametric Sensitivity

Parametric Sensitivity is a measure of change in performance (J) caused by the unit change in the value of a parameter for which a shape change occurs. For a CAD model, once the adjoint sensitivity (ϕ) and design velocity (V_n) due to perturbation of a CAD parameter are computed, the total change in objective function $(\mathrm{d}J)$ due to parametric perturbation can be predicted as the summation over the boundary as

$$\mathrm{dJ} = -\int_A \phi V_n dA\,. \tag{2.2}$$

Knowing the change in objective function due to the parametric perturbation in question, the parametric sensitivity (S), can then be calculated by normalizing this value with respect to the size of the perturbation which caused the design velocity as

$$\mathrm{S} = \frac{\mathrm{d}J}{\mathrm{d}P}. \tag{2.3}$$

3 PARAMETRIC EFFECTIVENESS

The parametric effectiveness was proposed in [32] as the ratio of the change in performance achieved by perturbing all the parameters in an optimum way (assumed here to be the steepest descent direction) subject to the constraint of a unit root-mean-squared boundary movement. When computing parametric effectiveness, a constraint on overall boundary movement is imposed for each parametric perturbation. This ensures a parameter moving an area of low sensitivity by a large amount or a small

movement of a large area of low sensitivity, would not be favored compared to the parameters causing a small localized movement in the areas of high sensitivity. Parametric effectiveness ranges from 0 to 1, and a high value of parametric effectiveness indicates that the parameters in the model can cause the shape to change close to the manner the adjoint sensitivity map suggests (i.e. each point on the model boundary moves proportional to the adjoint sensitivity on the model boundary). As the value of parameters approach their optimum values during the optimization, the parametric effectiveness tends to zero.

The detailed mathematical derivation of the measure can be found in [32]. A summary is that the optimum change in performance per root mean squared design velocity over the boundary for a model which is not constrained in the manner in which it can move by its parameterization can be predicted as

$$\left(\frac{dJ}{dV}\right)_{optimum} = -\sqrt{A\int_A \phi^2 dA}\,. \tag{4.1}$$

Assuming the optimum parametric performance improvement is obtained by perturbing the parameters in the direction of steepest decent, the vector of parameter changes can be written as

$$dP = k\{S_1 S_2 \dots \dots\}, \tag{4.2}$$

where k is a multiplier specifying the magnitude of the steepest decent vector. The optimum performance change per unit of root-mean-square design velocity, for a parameterized model is given by

$$\left(\frac{dJ}{dV}\right)_{param} = -\sqrt{\frac{A}{\int_A (\sum_{i=1}^{n} S_i V_{ni})^2\, dA}}\ \sum_{i=1}^{n} (S_i)^2\,, \tag{4.3}$$

The parametric effectiveness is given by

$$Parametric\ effectiveness = \frac{\left(\frac{dJ}{dV}\right)_{param}}{\left(\frac{dJ}{dV}\right)_{optimum}}. \tag{4.4}$$

The original work demonstrated the computation of design velocities for all parameters in a model, and that it was possible to identify a subset of parameters with higher parametric effectiveness than that of all parameters in the model. However, it was unable to suggest an automated approach which could be used to compute the parametric effectiveness of subset of parameters, or to identify the most effective set of parameters in industrially acceptable time-scales. In this work, an automated method to compute Parametric effectiveness is described, which allows its computation for any combination of CAD parameters. The method, shown in Algorithm 1, has been implemented in Python 3.5 for design velocities computed from CATIA V5 and SIEMENS NX, and adjoint sensitivity maps from HELYX [2].

4 AUTOMATED APPROACH FOR CAD PARAMETER SELECTION

It is shown in [32] that parameters selected based on parametric effectiveness are potentially better at localising the shape change in regions of high adjoint sensitivities compared to parameters selected based on having high sensitivities. It also states that the most effective set of parameters may not include all parameters, and it is suggested the subset of parameters could be identified using a power-set approach. Using a powerset requires the parametric effectiveness to be calculated for all possible combinations of parameters. While this could be achieved in a brute-force manner, the power-set of any set $\mathbb{Q}$ of p parameters are the set of all subsets of $\mathbb{Q}$ (including the empty set) giving a total of $2^p - 1$ different parametric combinations. The implementation of the power-set approach is therefore computationally prohibitive when number of parameters is large (as it is for most industrially relevant CAD models). In many cases it is likely that the cost of reducing the size of the set of parameters using a powerset approach would outweigh the benefit of reducing the number of parameters in the optimization.

Algorithm 1: Parametric Effectiveness Computation

Input: Parametric CAD model, adjoint sensitivity (ϕ)
Output: Parametric effectiveness for each CAD parameter

Generate STEP file for original model.
Perturb each parameter by small value ($\pm\epsilon$) and generate STEP files (p).
Generate surface facets for each STEP files ($p+1$) in GMSH.
Read surface facets for original and perturbed geometries.
for *parameter* $i \leftarrow 1$ **to** p **do**
    compute Design velocity (V_{ni})
    compute $S_i = \int \phi V_{ni} dA$
    compute $\sum_{i=1}^{p} S_i V_{ni}$, $\sum_{i=1}^{p} S_i^2$
    compute $\int (\sum_{i=1}^{p} S_i V_{ni})^2 dA$
    $(\frac{dJ}{dV})_{param} = \sqrt{\frac{A}{\int (\sum_{i=1}^{p} S_i V_{ni})^2 dA}} \sum_{i=1}^{p} S_i^2.$
$(\frac{dJ}{dV})_{optimum} = \sqrt{A \int \phi^2 dA}.$
parametric effectiveness $= \frac{(\frac{dJ}{dV})_{param}}{(\frac{dJ}{dV})_{optimum}}$

To reduce the cost of industrial optimization Design of Experiments based methodologies are popular, e.g. [22]. These are used to either screen out parameters predated to have a small influence on performance, and/or to generate response surfaces which are then used for optimization. The issue with these approaches are that they require many function evaluations to obtain sufficient data to formulate the process.

In this paper an efficient approach is formulated to efficiently obtain the optimum subset of parameters. This approach is more efficient than design of experiment approaches as it does not require multiple analyses (rather one primal and one adjoint evaluation is sufficient). Also, the process described below, which is akin to a greedy algorithm [8], means that there is no need to exhaustively evaluate Eqn. 4.3 for all parametric combinations. It is implement as

Step 1: All parameters with an individual parametric effectiveness greater than 0.02 are selected. The number of parameters $= m$. (It is assumed parameters with an individual parametric effectiveness smaller than 0.02 can be ignored).

Step 2: For the m parameters in Step 1, all the possible combinations of 2 parameters are created, each referred as a **set**. Here, $\mathbf{C}_2^m$ sets are formed, where $\mathbf{C}$ is a combinatorial operator. Sets are ordered with the parameter with the lowest numerical identifier as the first member.

Step 3: The sets are grouped together such that $m-1$ **groups** are created to contain parameter sets with the same first member. The parametric effectiveness of each set in each group is computed.

Step 4: The set with highest parametric effectiveness is selected for that group (and the other sets are deleted).

Step 5: For each group in Step 3, new sets are created by adding one of the remaining parameters to the set selected for each group in step 4.

Step 6: If the resulting parametric effectiveness calculated for a group in step 5 is less than that calculated for the same group in step 4, then the set from step 4 is selected and the new sets for that group are deleted and that group is considered complete. Else, Step 4 to Step 6 are repeated.

Step 7: when all groups are complete, the group containing the set with the maximum parametric effectiveness is identified. The parameters it contains are the subset of parameters which should be used to optimize the model

5 APPLICATIONS

5.1 Automotive ventilation Duct

A 3D parametric CAD model of an automotive ventilation duct from Volkswagen Group Research is shown in Figure 2a. The adjoint analysis was performed using the continuous adjoint approach [28], and the adjoint sensitivity map is shown in Figure 2b, which indicates that the regions shaded red should be pushed inward to reduce the objective function, while regions shaded blue should be pulled outward. The CAD model contains 263 real-valued parameters that can be perturbed to obtain a new shape of the duct.

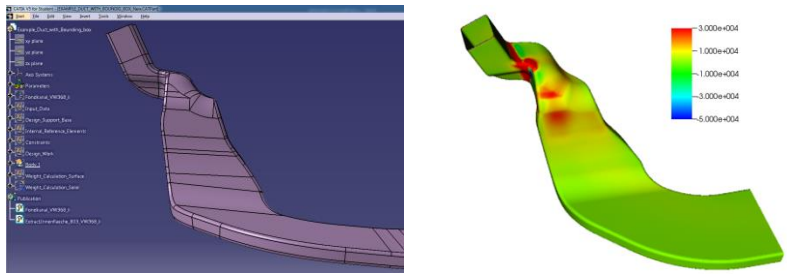

Figure 2: Automotive duct (a) parametric CAD model, (b) adjoint sensitivity map.

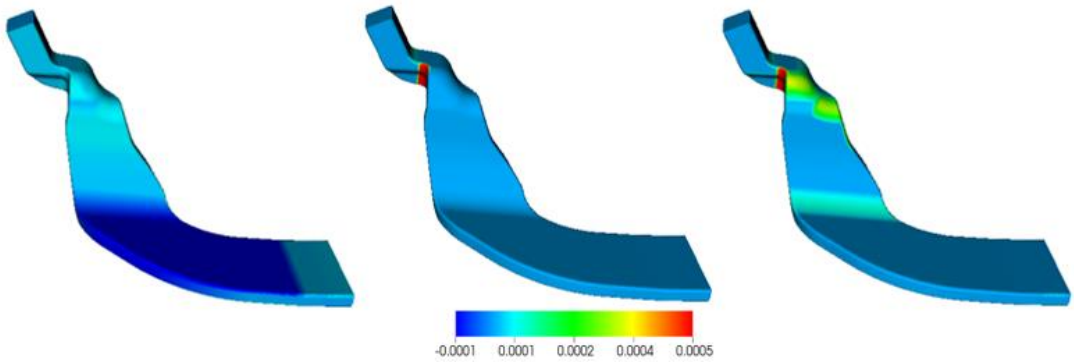

Figure 3: Design velocity for the overall boundary movement $dV = 1\,E^{-4}$, (a) all parameters, (b) designer's parameters, (c) most effective parameteric combination.

Here, the parametric effectiveness of two different sets of parameters was considered. The first set was a combination of four parameters that were selected by the designers to perturb the model mostly in the areas of high adjoint sensitivity [32]. This selection of parameters was based on the engineering judgement of the designer and their identification required considerable amount of time. The other parametric combination was that obtained using the approach presented in section 4. The parametric effectiveness of the parameters selected by designers was computed to be 0.47 compared to 0.53 for the most effective parametric combination (which consisted of 16 parameters). Interestingly, the parameters obtained using the described approach also contained the four parameters that were selected by the designers.

Figure 3 shows the contours of design velocity when all model parameters, the set of parameters selected by the designer, and the set of parameters calculated to have the highest parametric effectiveness were perturbed to move the boundary in the steepest decent direction. In all cases, the overall boundary movement is kept small ($dV = 1\,E^{-4}$). Figure 3c shows that the design velocity for the most effective parametric combinations move the model boundary in a manner close to that suggested

by the adjoint sensitivity map in Figure 2b, giving confidence in the applicability of the developed process.

5.2 S-Bend Duct

In the next test case, a parametric CAD model of the S-Bend duct is created in CATIA V5 as shown in Figure 4. It was modelled using eight 2D sketches at different positions and orientations along the length of the duct, and then developing a multi-section solid passing through these sketch profiles. The duct is composed of three individual sections i.e. inlet, S-Bend and outlet as shown in Figure 4. As the inlet and outlet ducts will join with other components their shape is fixed, so they are not considered for optimization. Here the optimization variables are the parameters defining the four sketches (shown in broken lines) describing the interior profile of the S-Bend (48 parameters).

The objective function considered for optimization is the power dissipation through the duct [28], defined as

$$J = \int_A v \cdot \hat{n} \left(p + \frac{1}{2} v^2 \right) dA \,, \tag{6.1}$$

where p and v are the pressure and velocity of the flow, and A and $\hat{n}$ are the surface of the duct and its unit normal, pointing away from the fluid area. The flow is laminar, with Reynolds number $R_e = 350$, calculated with a hydraulic diameter of $D_h = 0.053m$, inlet velocity $u = 0.1m/s$ and kinematic viscosity $v = 1.511\, X\, 10^{-5}\, m^2/s$. The computational mesh is created in ICEM-CFD [1] with approximately 250,000 hexahedral elements. The flow equations are solved using the standard steady state incompressible OpenFOAM© solver simpleFoam. The adjoint equations are solved using the adjoint solver provided by ENGYS® [21]. The adjoint surface sensitivities are shown in Figure 5, which suggests that red regions have to displaced away from the fluid, whereas regions shaded blue need to be displaced towards it.

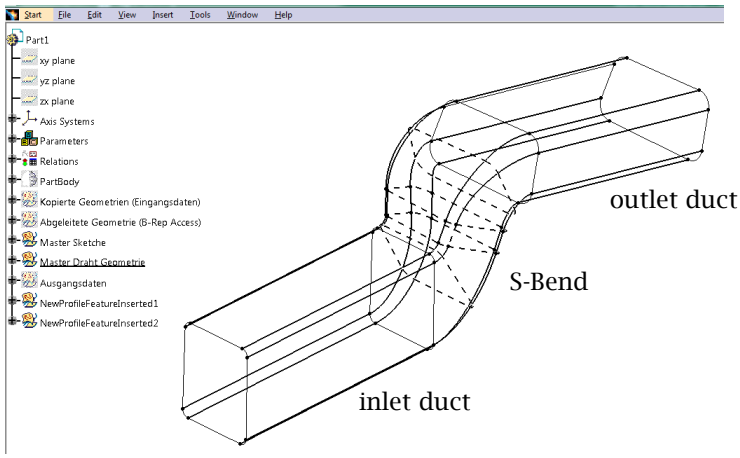

Figure 4: CAD model of S-Bend duct.

A CAD model with very large number of parameters would require a considerable amount of time to update if all parameters were updated during the parameterization, depending on the CAD modelling system. It is therefore beneficial to reduce the number of parameters to be used in optimization, providing there is a rationale for choosing which parameters to be used. Here the approach presented in section 4 is used to identify the subset of the full parameter set with the highest parametric effectiveness. In this test case, the most effective parameter set contained 13 parameters and had an effectiveness of 0.66 compared to an effectiveness of 0.60 obtained for all 48 parameters.

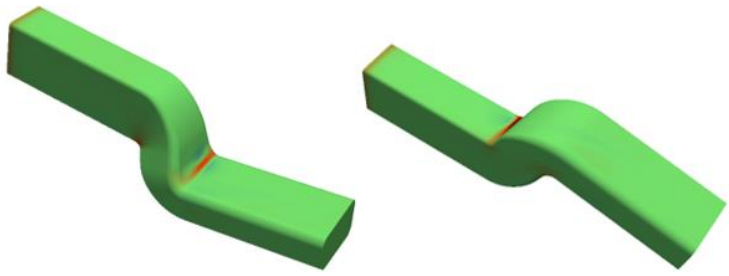

Figure 5: Adjoint sensitivity map: to minimize the objective function the surface should be pulled outwards at positive values (red) and pushed inwards at negative values (blue).

The computational effort required to update the S-Bend model in CATIA V5 using the different parameter sets is shown in Table 1, where it can be seen that updating all the parameters of the CAD model is comparatively more expensive compared to updating a selected set of parameters (factor of 4).

	Original CAD model (48 parameters)	Most effective parameter (13 parameters)
time for one CAD update	32 s	8 s

Table 1: Time required to update S-Bend CAD model.

5.2.1 Optimization

The shape of the S-Bend duct was optimized using the SLSQP method implemented in Scipy [3]. SLSQP is a gradient based optimization method which minimizes a function with any combination of bounds, equality and inequality constraints. For the S-Bend duct the optimization is performed using two different set of parameters, firstly using all the CAD parameters and secondly using the subset of parameters with the highest parametric effectiveness. At each optimization step, a new computational mesh is created in ICEM-CFD using an automated process. The optimization history for minimizing the power-loss across the duct is shown in Figure 6a. A reduction in power-loss by $10.72\,\%$ is observed when all the parameters are used for optimization, compared to $8.75\,\%$ when the parameters with highest parametric effectiveness are used. The total time required to optimize the model is higher when all parameters are used to update the CAD model compared to updating a subset of parameters (Figure 6b). It should be remembered that a CAD update is required for each iteration during the optimization, and that the process of CAD model updating cannot be parallelized.

Table 2 shows the total time taken by SLSQP optimization for two different sets of parameters. Even for this relatively simple test case, with a reasonably smaller number of design parameters, reducing the number of parameters for optimization resulted in a time saving of approximately 9,000 seconds (a 29% reduction). The reduction in the gain in performance was approximately 2% (Figure 6a).

5.3 DrivAer Model

In the next test case, the developed framework is applied to an automotive noise reduction problem, with the use of a surrogate model for aeroacoustics [31]. The model under investigation is the TUM DrivAer vehicle [11], using a fast-back configuration with smooth underbody and closed wheels. Here, the CAD model of the car mirror was originally provided as a STEP file. This is a CAD translation standard that does not include any features or parameters. A replica model was created using CATIA V5 using a series of points, lines and splines. The wireframe model of the mirror is shown in Figure 7. The surface fitting methods in CATIA V5 (like multi-section surface and fill surface) are then used to

create the outer surfaces and produce 3D CAD model of the mirror with 2925 CAD parameters. The parameters are the x, y and z positions of the point in Figure 7 and the resulting geometry is shown in Figure 8.

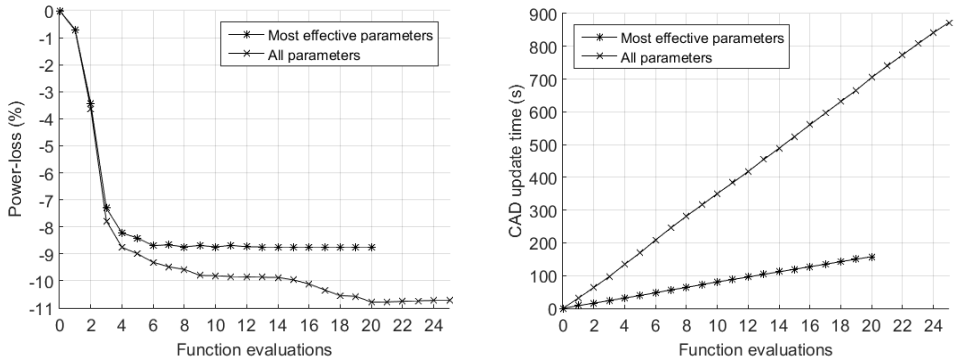

Figure 6: Optimization of S-Bend duct, (a) change in objective function, (b) time taken to update CAD model.

	Original CAD model (48 parameters)	Most effective parameter (13 parameters)
total time taken for updating CAD during the optimization	873 s	165 s
total time for optimization	31360 s	22375 s

Table 2: Time statistics for S-Bend optimization.

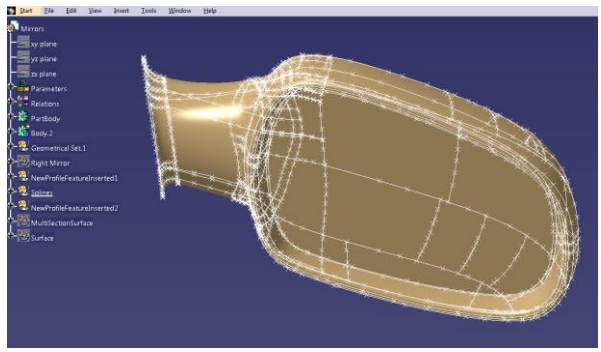

Figure 7: Parametric CAD model of car mirror (wireframe).

Here the optimization process alters the shape of the mirror geometry, targeting a shape which transmits less noise to the interior of the car. The low frequency noise perceived inside the cabin can be linked to the turbulence level at the area directly outside of the driver side window as shown in Figure 9.

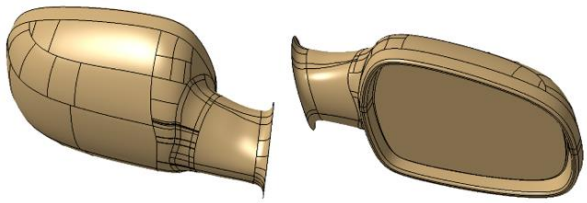

Figure 8: CAD model of car mirror (solid).

Figure 9: Volume (in red) over which the objective function is integrated. The volume was created by the extrusion of the DrivAer driver window by 3 cm.

A surrogate aeroacoustics objective function can be formulated as the integral of the turbulent viscosity squared over a volume near the side window as

$$F_{noise} = \int_{\Omega} \nu_t^2 \, d\Omega, \tag{6.1}$$

where ν_τ is the turbulent viscosity. It is important to note that without the differentiation of the turbulence model, relying on the "frozen turbulence" assumption, dealing with an optimization problem of this kind would not be possible. This is because the objective function itself depends on the turbulent variable $\tilde{\nu}$.

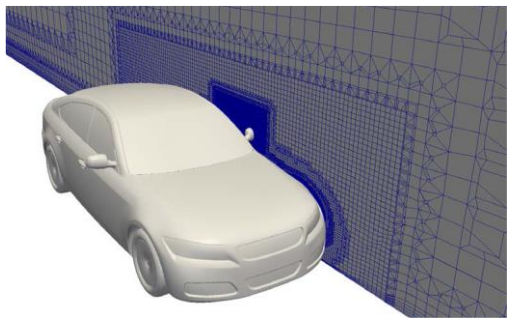

Figure 10: Slice of the computational grid around the DrivAer vehicle.

For the flow and adjoint analysis half of the car was meshed. The computational grid consisted of 5 million cells. As seen in Figure 10, a grid refinement is used around the mirror for a better turbulence resolution in this area. The flow equations were solved using the standard steady state incompressible OpenFOAM© solver simpleFoam. In this case, the adjoint equations were enhanced with the fully differentiated Spalart-Allmaras turbulence model based on wall functions, developed by Prof. Giannakoglou's research group [30]; without the differentiation of the turbulence model, relying on

the "frozen turbulence" assumption, dealing with an optimization problem of this kind would not be possible, because the objective function itself depends on the turbulent variable $\tilde{\nu}$. Finally, the adjoint system was solved using the HELYX Adjoint solver, provided by ENGYS [21].

The adjoint sensitivity map computed at the first optimization cycle is presented in Figure 11, where red areas must be pushed inward while blue are to be pulled outward to reduce the objective function. Now, the approach described in section 4 was used to compute the most effective parameter set consisting of 48 parameters with parametric effectiveness of 0.79. The benefit of this reduction in terms of computational effort required to update the parametric DrivAer model in CATIA V5 is shown in Table 3, where a single update of the CAD model using all parameters is computationally much more expensive (83 times more) than using the subset.

	Original CAD model (2925 parameters)	Most effective parameter (48 parameters)
CAD update time	10716 s	129 s

Table 3: Time required to update the DrivAer CAD model.

By comparison, an alternative approach to reducing the number of parameters would be to select those with the highest parametric sensitivity. Figure 12 compares the design velocities when the model is perturbed using all 2925 parameters (Figure 12(a)), the most effective parametric combination consisting of 48 parameters (Figure 12(b)), and the same number of parameters with highest parametric sensitivities (Figure 12(c)). In all cases the parameters are perturbed in the steepest decent direction and the overall boundary movement caused by the perturbations is kept constant ($dV = 3E^{-5}$). It is seen that the parametric combination with highest parametric effectiveness moves the model such that the boundary displacement is highly focused in the areas of high adjoint sensitivity and very little in other regions, while using the most sensitive parameters moves the boundary of the model in less focused fashion.

Figure 11: Sensitivity maps targeting at turbulent noise minimization as seen from top and bottom.

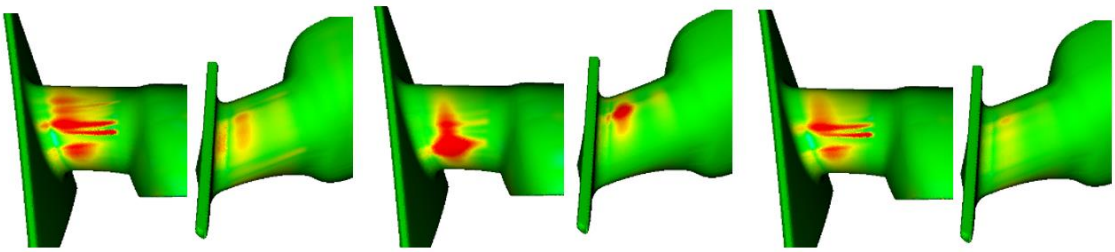

Figure 12: Design velocity for the overall boundary movement $dV = 3E^{-5}$, (a) All parameters, (b) most effective parameteric combination, (c) most sensitive parameters.

5.3.1 Optimization

The shape optimization of car mirror was performed for both the models parameterized using the parameter set with the highest parametric effectiveness and that with the 48 parameters with highest parametric sensitivities. A steepest descent strategy was used to update the design variables during the optimization. For each optimization step, design velocity method described in section 2 was used to deform the surface mesh points, and the nodes of the internal mesh were displaced by solving a Laplace equation [20]. After the optimization algorithm converged, the optimal geometry was 6.8% "quieter" when using the most effective parametric combination, compared to 4.1% when the 48 most sensitive parameters were used. Comparing the design velocity of the optimized designs for the most effective parameters (Figure 13), it is seen that the top and bottom of the neck of the mirror has been pushed in to suppress the generation of turbulence on the wake of the mirror, consequently reducing the turbulence viscosity flowing through the volume over which the objective function is integrated (Figure 14).

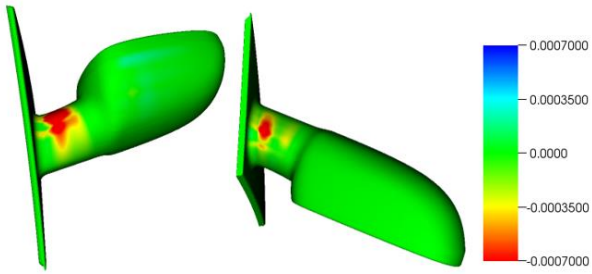

Figure 13: Comparison between the original and optimized CAD model for the most effective parametric combination.

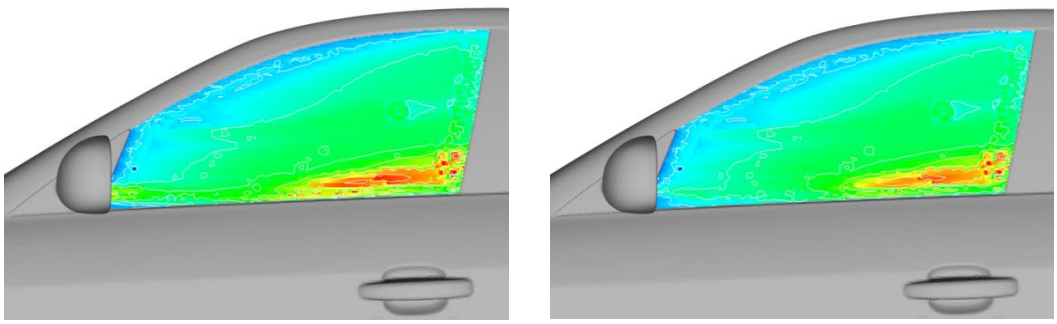

Figure 14: Squared turbulent viscosity computed at a slice of the volume over which the objective function is integrated. (starting geometry left, optimized right).

6 DISCUSSION

This work presented an automated "greedy algorithm" approach to compute the parametric effectiveness for all possible sets of parameters defined within a CAD modelling system, and to select optimum combination of parameters to be used for optimization. The main benefit of the approach is that the parameters can be down selected based on one computational analysis and one adjoint analysis. This is much cheaper than alternative approaches which require many analyses to be carried out.

For the automotive duct, using all 263 parameters in the model showed a significantly lower parametric effectiveness compared to that obtained for the most effective set of parameters.

Interestingly, the parameters which appeared to the designers to perturb the model in the areas of high adjoint sensitivity had a comparatively lower parametric effectiveness compared to the ones obtained using the developed approach. It was also demonstrated that the parameters selected using the presented approach were potentially better at localizing the shape change in regions of high adjoint sensitivities. It is to be noted that the parameters selected by designers were based on engineering judgement and required a considerable amount of skill and time to identify. Also, the parameters obtained using the automated process contained the parameters that were selected by the designers, which substantiates the applicability of the developed approach to reduce the workload of designers to select the optimum parameters to be used for optimization. For the S-Bend duct model where the number of design parameters was small (48 parameters) it was shown that using the methodology described in section 4, smaller set of design parameters with higher parametric effectiveness can be selected. This resulted in time saving of approximately 700 seconds resulting from updating the CAD model at each optimization step. It was shown that, using parametric effectiveness a trade-off can be made between the available computational resource and the achievable performance gain.

The application of developed methodologies to the optimization of DrivAer model demonstrated that in some scenarios updating the CAD model of high complexity is computationally very expensive and each update may require more time than that required for CFD analysis. The CAD update at one optimization step was completed in approximately 3 hours (on a 3.60GHz workstation with 16GB RAM), while the primal and adjoint analysis took approximately 1 hour (on a high-performance cluster (HPC) with 216 computers) each for primal and adjoint analysis. In an industrial environment, it is less likely that a CAD system used for creating these designs is installed on an HPC, and thus the process of updating the CAD model is to be performed on a normal workstation, as shown in this paper.

The approach described in section 4 was then used to reduce the design space of the DrivAer model and obtain 48 parameters with highest parametric effectiveness of 0.79. It was found that these set of parameters had significantly higher parametric effectiveness than the one obtained when the same number of most sensitive parameters were analyzed. Also, it should be noted that these parameters were not the ones with highest individual parametric effectiveness. This demonstrated that it was not efficient to use the parametric sensitivity and effectiveness of individual parameters as the sole criterion for selecting the optimum combination of parameters for optimization. The findings were strengthened by comparing the optimization results, where the most effective parametric combination performed substantially better for minimization of the selected objective function.

Parametric effectiveness is a measure of how good a parameterization strategy is for the purposes of optimization. Where it is high a designer can have confidence in the parameterization strategy used. Where it is low it indicates that it may be beneficial to update the parameters before carrying out an optimization. In the future, the approach could be used to determine when new parameters are needed on a model and be used to compare the advantages offered by the insertion of different parameters to the model. This provides a rational metric for comparing different parameterization strategies *a priori* to the optimization process.

7 CONCLUSIONS

From this work following conclusions have been drawn

- An automated approach was developed to rate the quality of different sets of CAD parameters and was used to select the optimum combination of parameters to be used for optimization.
- The rationale behind using the developed approach is outlined in terms of time required to update a parametric CAD model during the optimization, which is an important factor to be considered when using the optimization process in an industrial workflow.

8 ACKNOWLEDGEMENTS

This work has been conducted within the IODA project (http://ioda.sems.qmul.ac.uk), funded by the European Union HORIZON 2020 Framework Programme for Research and Innovation under Grant Agreement No. 642959.

Dheeraj Agarwal, http://orcid.org/0000-0001-5340-5851
Trevor T. Robinson, http://orcid.org/0000-0002-6595-6308
Cecil G. Armstrong, http://orcid.org/0000-0001-8695-5016

REFERENCES

[1] ICEM-CFD, http://www.ansys.com/en-GB/Services/training-center/platform/introduction-to-ansys-icem-cfd-Hexa.
[2] HELYX, http://engys.com/products/helyx.
[3] Scipy Optimize, https://docs.scipy.org/doc/scipy/reference/optimize.html.
[4] Agarwal, D.; Robinson, T. T.; Armstrong, C. G.; Marques, S.; Vasilopoulos, I.; Meyer, M.: Parametric design velocity computation for CAD-based design optimization using adjoint methods, Engineering with Computers, 34(2), 2018, 225-239. http://dx.doi.org/10.1007/s00366-017-0534-x.
[5] Belegundu, A.; Rajan, S.: A shape optimization approach based on natural design variables and shape functions, Computer Methods in Applied Mechanics and Engineering, 66(1), 1988, 87-106. https://doi.org/10.1016/0045-7825(88)90061-8.
[6] Burgos, M. J.: NURBS-Based Geometry Parameterization for Aerodynamic Shape Optimization, Telecomunicacion, 2015.
[7] Chen, S.; Torterelli, D.: Three-dimensional shape optimization with variational geometry, Structural Optimization, 13, 1997, 81-94. https://doi.org/10.1007/BF01199226.
[8] Cormen, T. H.; Leiserson, C. E., Rivest, R. L., Stein, C.: Greedy Algorithms, Chapter 16. In: Anonymous Introduction to algorithms, The MIT Press, 2001.
[9] Giles, M. B.; Pierce, N.: An introduction to the adjoint approach to design, Flow, Turbulence and Combustion, 65, 2000, 393-415. https://doi.org/10.1023/A:1011430410075.
[10] Hardee, E.; Chang, K.; Tu, J.; Choi, K. K.; Grindeanu, I.; Yu, X.: A CAD-based design parameterization for shape optimization of elastic solids, Advances in Engineering Softwares, 30, 1999, 185-199. https://doi.org/10.1016/S0965-9978(98)00065-9.
[11] Heft, A. I.; Indinger, T.; Adams, N.: Experimental and numerical investigation of the DrivAer model, ASME 2012 Fluids Engineering Summer Meeting, Rio Grande, Puerto Rico, 2012. https://doi.org/10.1115/FEDSM2012-72272.
[12] Helgason, E.; Krajnovic, S.: Aerodynamic shape optimization of a pipe using the adjoint method, ASME International Mechanical Engineering Congress & Exposition, Nov, 2012.
[13] James, K. A.; Lee, E.; Martins, J. R.: Stress-based topology optimization using an isoparametric level set method, Finite Elements in Analysis and Design, 58, 2012, 20-30. https://doi.org/10.1016/j.finel.2012.03.012.
[14] James, K. A.; Martins, J. R.: An isoparametric approach to level set topology optimization using a body-fitted finite-element mesh, Computers & Structures, 90, 2012, 97-106. https://doi.org/10.1016/j.compstruc.2011.10.004.
[15] Jameson, A.: Aerodynamic shape optimization using the adjoint method, Lectures at the Von Karman Institute, Brussels, 2003, .
[16] Jameson, A.: Efficient aerodynamic shape optimization, AIAA paper, 4369, 2004, 2004.
[17] Jameson, A.; Martinelli, L.; Pierce, N.: Optimum aerodynamic design using the Navier–Stokes equations, Theoretical and Computational Fluid Dynamics, 10(1), 1998, 213-237.
[18] Jesudasan, R.; Zhang, X.; Mueller, J.: Adjoint optimisation of internal turbine cooling channel using NURBS-based automatic and adaptive parametrisation method, ASME Gas Turbine Conference, GTIndia2017-4669, 2017.

[19] Kammerer, S.; Mayer, J.; Paffrath, M.; Wever, U.; Jung, A.: Three-dimensional optimization of turbomachinery bladings using sensitivity analysis, ASME Paper GT2003-38037, 6, 2003, 1093-1101. https://doi.org/10.1115/GT2003-38037.
[20] Kapellos, C.; Alexias, P.; Villiers, E. d.: *The adjoint method for automotive optimization using a sphericity based morpher*, NAFEMS adjoint CFD Seminar 2016, 2016.
[21] Karpouzas, G. K.; Papoutsis-Kiachagias, E. M.; Schumacher, T.; Villiers, E. d.; Giannakoglou, K. C.; Othmer, C.: Adjoint optimization for vehicle external aerodynamics, International Journal of Automotive Engineering, 7(1), 2016, 1-7. https://doi.org/10.20485/jsaeijae.7.1_1.
[22] Kefi, S.; Joneja, A.; KT Tse, T.; Li, S.: Channel geometry optimization for vertical axis wind turbines in skyscrapers, Computer-Aided Design and Applications, 15(2), 2018, 211-218. https://doi.org/10.1080/16864360.2017.1375671.
[23] Koch, J.; Papoutsis-Kiachagias, E.; Giannakoglou, K.: Transition from adjoint level set topology to shape optimization for 2D fluid mechanics, Computers & Fluids, 150, 2017, 123-138. https://doi.org/10.1016/j.compfluid.2017.04.001.
[24] Kripac, J.: A mechanism for persistently naming topological entities in history-based parametric solid models, Computer-Aided Design, 29(2), 1997, 113-122. https://doi.org/10.1145/218013.218024.
[25] Mader, C. A.; RA Martins, J.; Alonso, J. J.; Der Weide, E. V.: Adjoint: an approach for the rapid development of discrete adjoint solvers, AIAA Journal, 46(4), 2008, 863-873. https://doi.org/10.2514/1.29123.
[26] Martin, M. J.; Andrés, E.; Widhalm, M.; Bitrián, P.; Lozano, C.: Non-uniform rational B-splines-based aerodynamic shape design optimization with the DLR TAU code, Proceedings of the Institution of Mechanical Engineers, Part G: Journal of Aerospace Engineering, 226(10), 2012, 1225-1242. https://doi.org/10.1177%2F0954410011421704.
[27] Othmer, C.: Adjoint methods for car aerodynamics, Journal of Mathematics in Industry, 4, 2014, 1-23. https://doi.org/10.1186/2190-5983-4-6.
[28] Othmer, C.: A continuous adjoint formulation for the computation of topological and surface sensitivities of ducted flows, International Journal for Numerical Methods in Fluids, 58(8), 2008, 861-877. https://doi.org/10.1002/fld.1770.
[29] Papadimitriou, D.; Giannakoglou, K.: Total pressure loss minimization in turbomachinery cascades using a new continuous adjoint formulation, Proceedings of the Institution of Mechanical Engineers, Part A: Journal of Power and Energy, 221(6), 2007, 865-872. https://doi.org/10.1243/09576509JPE463.
[30] Papoutsis-Kiachagias, E.; Giannakoglou, K. C.: Continuous adjoint methods for turbulent flows, applied to shape and topology optimization: industrial applications, Archives of Computational Methods in Engineering, 23(2), 2016, 255-299. https://doi.org/10.1007/s11831-014-9141-9.
[31] Papoutsis-Kiachagias, E.; Magoulas, N.; Müller, J.; Othmer, C.; Giannakoglou, K. C.: Noise reduction in car aerodynamics using a surrogate objective function and the continuous adjoint method with wall functions, Computers & Fluids, 122, 2015, 223-232. https://doi.org/10.1016/j.compfluid.2015.09.002.
[32] Robinson, T. T.; Armstrong, C. G.; Chua, H. S.: Determining the parametric effectiveness of a CAD model, Engineering with Computers, 29(1), 2013, 111-126. https://doi.org/10.1007/s00366-011-0248-4.
[33] Thomas, S.; Carsten, O.: Adjoint optimization for vehicle external aerodynamics, International Journal of Automotive Engineering, 7(1), 2016, 1-7. https://doi.org/10.20485/jsaeijae.7.1_1.
[34] Walther, B.; Nadarajah, S. K.: Adjoint-based constrained aerodynamic shape optimization for multistage turbomachines, Journal of Propulsion and Power, 31(5), 2015, 1298-1319. https://doi.org/10.2514/1.B35433.
[35] Wang, M. Y.; Wang, X.; Guo, D.: A level set method for structural topology optimization, Computer Methods in Applied Mechanics and Engineering, 192(1), 2003, 227-246. http://dx.doi.org/10.1016/S0045-7825(02)00559-5.

[36] Xu, S.; Jahn, W.; Müller, J.: CAD based shape optimization with CFD using a discrete adjoint, International Journal of Numerical methods in Fluids, 74, 2014, 153-168. https://doi.org/10.1002/fld.3844.
[37] Xu, S.; Radford, D.; Meyer, M.; Müller, J.: CAD-based adjoint shape optimisation of a one-stage turbine with geometric constraints, ASME Turbo Expo, 2015. https://doi.org/10.1115/GT2015-42237.
[38] Xu, S.; Timme, S.; Mykhaskiv, O.; Müller, J.: Wing-body junction optimisation with CAD-based parametrisation including a moving intersection, Aerospace Science and Technology, 68, 2017, 543-551. https://doi.org/10.1016/j.ast.2017.06.014.
[39] Yu, G.; Müller, J.; Jones, D.: CAD based shape optimization using adjoint sensitivities, Computers and Fluids, 46, 2011, 512-516. https://doi.org/10.1016/j.compfluid.2011.01.043.